Nonlinear Fragility Analysis of Three Different Concrete Bridge Mid-Column Structural Types

Miloš Čokić [1] ✉, *Radomir Jovo Folić* [2], *Jovan Ćiro Drča* [1], *Boris Radomir Folić* [3]
✉ e-mail: cokicmilos@gmail.com
[1] Termoenergo inženjering, Bulevar kralja Aleksandra 298, Belgrade, Republic of Serbia
[2] University of Novi Sad, Faculty of Technical Sciences, Novi Sad, Republic of Serbia
[3] University of Belgrade Faculty of Mechanical Engineering, Innovative Centre, Belgrade, Republic of Serbia
DOI: https://doi.org/10.14459/icbdb24.37

Abstract Reinforced concrete (RC) road bridges play a crucial role in transportation infrastructure and must endure varying degrees of damage during seismic events, including the risk of collapse. Their resilience is vital for post-earthquake recovery, enabling the movement of emergency services and goods. While some bridges may require repairs, many can still accommodate emergency vehicles. This study focuses on the seismic assessment of bridges, particularly those built under outdated regulations, guided by European standards such as EN 1998. This paper presents a comparative numerical analysis of three bridge models with identical superstructures but varying substructures, specifically the mid-columns. The analyzed prestressed concrete bridges span 88 meters and adhere to European standards. By employing nonlinear analysis methods, the study assesses how design variations influence seismic fragility and column responses. Key findings reveal that design choices significantly affect structural performance, highlighting the need for rigorous seismic evaluations. Fragility curves indicate that Model 1, despite strong initial resilience, exhibits increased vulnerability under severe conditions. In contrast, Models 2 and 3 demonstrate enhanced resilience, especially in extensive and complete damage states. This analysis emphasizes the importance of ductility in bridge design, with Model 2 proving particularly effective for regions prone to high seismic activity. Overall, the study underscores the necessity for continuous optimization of bridge designs to mitigate seismic risks and ensure safety and functionality during and after earthquakes.

1 Introduction

Reinforced concrete (RC) road bridges are vital to transportation networks and can sustain various levels of damage during strong earthquakes, including potential collapse. Their resilience is crucial for post-earthquake mobility, as they facilitate the movement of goods and people after disasters. While some bridges may need repairs, many remain usable for emergency vehicles [1]. Chapter 7 of the book [2] addresses the seismic assessment of existing buildings, applicable to bridges

built under older regulations. In Europe, EN 1998 [3] guides the assessment and design of bridges, Seismic vulnerability and fragility are further discussed in [4-6].
The advancement of performance-based seismic design (PBSD) is enhancing the service life of bridges. Recent developments focus on improving post-earthquake functionality and accurately predicting seismic performance across various scenarios. Establishing performance criteria is essential for applying PBSD to unique hazards [7]. Damage limit states play a crucial role in this design approach, where damage control indicates repairable damage and collapse prevention aims to avoid non-repairable damage [8]. The design philosophy in EN1998-2 [3] emphasizes maintaining structural integrity and communication post-earthquake. It aims to achieve two key goals:

- Non-collapse (ultimate limit state – ULS) ensures the bridge retains structural integrity after a seismic event, even if some damage occurs.

- Minimization of damage (serviceability limit state – SLS) allows only minor damage to secondary components during frequent earthquakes.

Unlike buildings, where nonlinear hinges form in columns to prevent failure, bridges should maintain superstructures in the linear-elastic zone.
This paper presents a comparative numerical analysis of three bridge models (**Figures 1-3** which have identical super-structures but different sub-structures, specifically the supporting mid-columns. The analyzed prestressed concrete bridges span 88 meters and they are located on the same site. The design solutions for the frame structural system were selected based on terrain characteristics and project requirements, adhering to European standards EN1990 [9], EN1991 [10], EN1992 [11], and EN1998-2 [3]. Each bridge has two lanes (3.50 m width) and two pedestrian paths (1.5 m width), with spans of 24.0+40.0+24.0m. The substructure includes RC columns with foundations and a prestressed beam with a variable-height box cross-section (1.40m to 2.60m), cast in situ. The paper analyzes how these design choices impact seismic fragility and bridge column responses using nonlinear analysis methods. Structural damage can lead to significant material loss, compromising the bridge's functions and posing risks to nearby areas. Therefore, damage limit states and fragility curves were calculated using nonlinear dynamic analysis and earthquake time-history data. The structural responses of bridge columns were compared across different damage states, contributing to the assessment of seismic damage and resilience. The findings enhance understanding of how various design factors affect the seismic response and fragility of the bridge structural system.

2 Methodology of the analysis and structural modelling

2.1 Geometric and Material Properties of the Structure

In Model 1 (M1) in **Figure 1**, the mid-columns are massive and designed as DCL and in models 2 (**Figure 3**) and 3 (**Figure 4**) (M2 and M3), the mid-columns are designed as DCM elements.

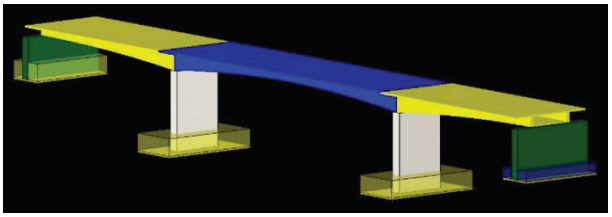

Figure 1: Bridge model 1 (M1), [12]

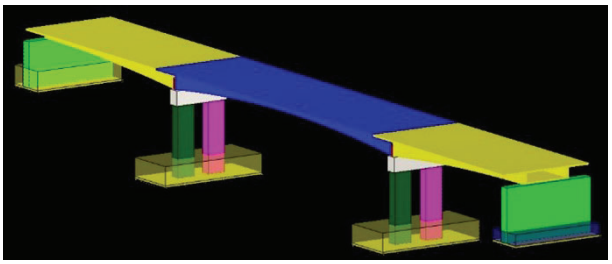

Figure 2: Bridge model 2 (M2), [12]

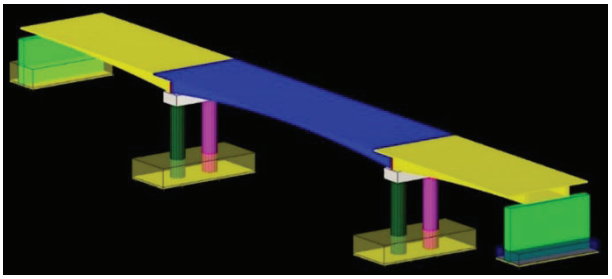

Figure 3: Bridge model 3 (M3), [12]

For M2 and M3, the mid-columns construction comprises three elements. These consist of two piers and a crossbeam, which are rigidly connected to the main deck. In M2, the mid-columns have a rectangular cross-section, while in M3, the mid-columns have a circular cross-section. The crossbeams have a rectangular cross-section. The bridge structures are of the rigid frame type, restrained perpendicular to the bridge alignment at the abutments. The mid-columns are fixed at the bottom and they all have a height of HC = 8.45 m. Concrete of grade C30/37 and steel B500 for reinforcement were used in calculation. The bridge mid-columns in M1, M2, and M3 were designed in accordance with the European standards [3], [9-11]. The calculations were carried out using the software packages Radimpex Tower [12] (linear analysis), CSi SAP2000 [13] (damage limit state thresholds calculation), and Seismosoft Seismostruct [14] (nonlinear analysis).

The assessment of damage limit states in the mid-columns was conducted on three different models to compare and analyze the values at which these damage limit states (LS) occur. The current modeling approach of analyzed structures (**Table 1**) provides a balanced framework for the assessment of bridge performance, with nonlinear analysis of critical components (mid-columns) and simplified modeling of other structural elements. The **Table 2** provides a detailed comparison of the geometric and material properties of the mid-columns in each model.

Table 1: Structural element type used in the models.

Element	Structural element type in the models
Mid-column	Nonlinear element with hinges
Mid-column foundation	Restraints
Cross-beam	Linear element
Bridge deck	Linear element
Abutments	Restraints

Table 2: Structural element type used in the models.

Cross-section properties	M1	M2	M3
Ductility class:	DCL (q = 1.5)	DCM (q = 3.0)	DCM (q = 3.0)
Crossbeam:	/	d/b/l = 1.2/1.6/6.2m	d/b/l = 1.2/2.4/6.2m
Height: d [m]	6.0	2.0	Diameter D = 1.6m
Width: b [m]	1.2	1.0	
Longitudinal rebars in columns:	132 Ø25 A_s = 648.12 cm^2	32 Ø14 A_s = 49.28 cm^2	36 Ø14 A_s = 55.44 cm^2
Stirrups in column:	Ø12/15, Confinement bars: 4 x 7	Ø12/15, Confinement bars: 4 x 6	Ø12/15, Confinement bars: 1 hoop

2.2 Damage limit state performance points

Table 3 defines different levels of damage and their threshold values for the mid-columns of the bridge models and how these thresholds are used to evaluate the structural performance. To determine the damage limit LS values, a nonlinear static analysis (NSA) and incremental nonlinear dynamic analysis (NDA) were performed. By analysing the response of the structures, the damage states for various conditions were assessed. Similar approach to the definition of damage or limit state values is used in paper [15].

2.3 Nonlinear dynamic analysis

Nonlinear time-history analysis (THA) is conducted by using seven particular accelerograms in only one direction, perpendicular to the bridge deck alignment, because of its simplicity and the wide application of this method of analysis.

The accelerograms shown in **Figure 4** and **Table 4** were chosen from the ORFEUS database [16] and scaled to match elastic response spectra for a 10% exceedance probability over 50 years at a ground acceleration of 0.1g. Records were selected based on a minimum magnitude of 5.5Ms (type 1 RS) and correspond to soil type E. The REXELite tool [16].was used to find waveforms compatible with the target spectrum The selection process ensured that the scaled records matched the elastic response spectrum used in the bridge design. Scaled accelerograms are applied in nonlinear dynamic analysis (NDA) with a scaling range of 0.1g–1.0g, in increments of $\Delta PGA = 0.1g$.

Table 3: Description of the damage state threshold values

Nr.	Limit state (LS)	Description	M1	M2	M3
1)	**Small damage (SD)**	Depends on steel and concrete values. SD occurs either in the first step, when reaching the reinforcement yield limit ($\varepsilon_s \geq \varepsilon_{sy}$) or the stress limit of concrete with maximum strength in the protective layer of concrete ($\varepsilon_c \geq \varepsilon_{c1}$).	$\varepsilon_s \geq \varepsilon_{sy} = 0.0025$ *or* $\varepsilon_c \geq \varepsilon_{c1} \approx 0.002$		
2)	**Moderate damage (MD)**	This level of damage is assumed to occur when reaching the stress limit in the protective layer of concrete ($\varepsilon_c \geq \varepsilon_{cu,1}$) or the maximum stress of the confined concrete core ($\varepsilon_{c,c} \geq \varepsilon_{cc,1}$)	$\varepsilon_c \geq \varepsilon_{cu,1} = 0.0035$ *or* $\varepsilon_{c,c} \geq \varepsilon_{cc,1} = 0.0030$	$\varepsilon_c \geq \varepsilon_{cu,1} = 0.0035$ *or* $\varepsilon_{c,c} \geq \varepsilon_{cc,1} = 0.0034$	$\varepsilon_c \geq \varepsilon_{cu,1} = 0.0035$ *or* $\varepsilon_{c,c} \geq \varepsilon_{cc,1} = 0.0026$
3)	**Extensive damage (ED)**	Occurs in the first step, when the ultimate stress is reached in the confined concrete core ($\varepsilon_{c,c} \geq \varepsilon_{cc,u}$).	$\varepsilon_{c,c} \geq \varepsilon_{cc,u} = 0.0069$	$\varepsilon_{c,c} \geq \varepsilon_{cc,u} = 0.0129$	$\varepsilon_{c,c} \geq \varepsilon_{cc,u} = 0.0078$
4)	**Complete damage (CD)**	This state results in the case of tensile fracture of longitudinal reinforcement bars ($\varepsilon_s \geq \varepsilon_{s,u}$)., the mid-column drift reaches ($\theta \geq \theta_u$) and the loss of system balance.	$\varepsilon_s \geq \varepsilon_{s,u} = 0.05$ *or* $\theta \geq \theta u$		

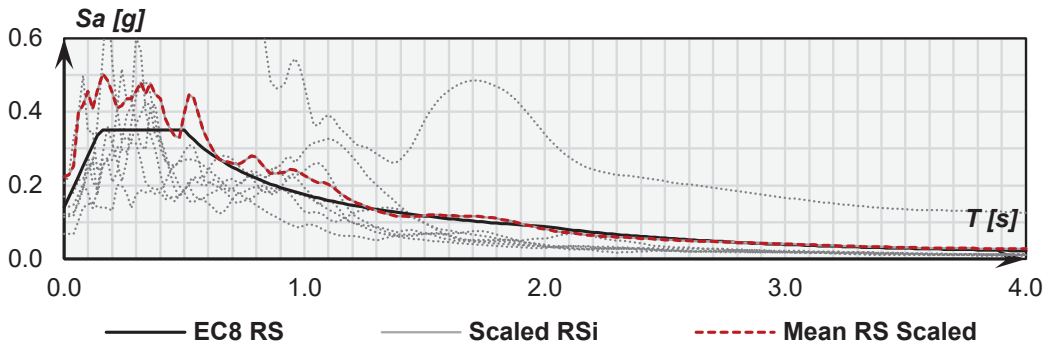

Figure 4: Response spectra used in the analysis (scaled RSi, mean RS and mean scaled RS)

Table 4: Main properties of the earthquakes that were used in NDA

Event ID	Event date and time	Mw	Epicentral distance [km]	PGA [cm/s^2] (component)
EMSC-20161030_0000029	2016-10-30T06:40:18	6.6	27.6	110.78 (E)
EMSC-20161030_0000029	2016-10-30T06:40:18	6.6	27.6	167.58 (N)
IT-1976-0002	1976-05-06T20:00:12	6.4	41.6	61.59 (N)
EMSC-20160824_0000006	2016-08-24T01:36:32	6.0	45.5	128.78 (N)
IT-1997-0006	1997-09-26T09:40:24	6.0	4.8	223.38 (E)
UZ-1976-0001	1976-05-17T02:58:40	6.7	3.4	708.03 (E)
EMSC-20161026_0000095	2016-10-26T19:18:06	5.9	32.5	115.29 (E)

3 Discussion of results

3.1 Damage limit states

The NSA results are shown in Figure 5, detailing force and displacement values, while Figure 6 compares NSA and NDA outcomes. Notation Mi,s indicates drift values from NSA, and Mi,d denotes those from NDA. The analysis reveals that the mid-columns in M2 and M3, designed with higher ductility, perform better in damage tolerance than M1. Differences in cross-sectional shapes and reinforcement also impact their responses to loading. M1, with massive mid-columns designed as DCL, shows the lowest drift values for SD and MD states, indicating robust performance. In contrast, M2 and M3, designed as DCM, exhibit higher drift values, especially in ED and CD states, suggesting reduced structural integrity under severe conditions. While M2 has lower drift than M3 for ED and CD, both surpass M1, highlighting the significance of design in mitigating damage. M1 requires less force than M2 to reach ED and CD states, indicating it is more resilient initially but less robust overall compared to M2, which demands the highest force to reach damage states, reflecting its superior capacity. M3 performs well in the ED state but is less effective than M2 in the CD state, requiring less force than M2 while outperforming M1 in certain cases.

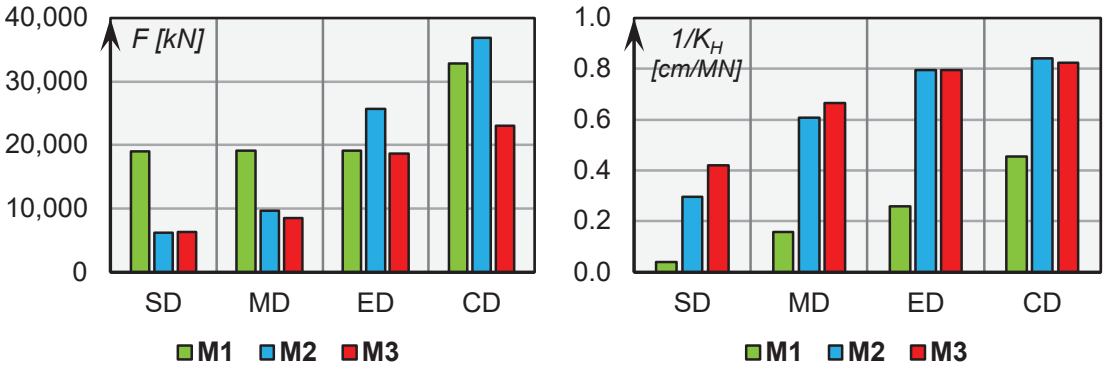

Figure 5: Comparison of force values (left) and 1/KH (stiffness) of mid-column for M1, M2 and M3, derived from NS

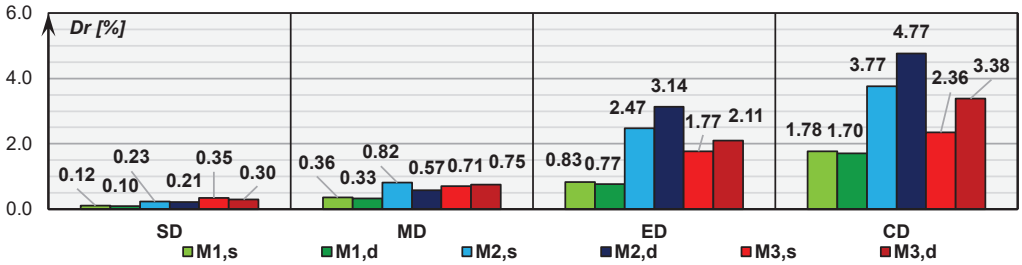

Figure 6: Comparison of force values (left) and 1/KH (stiffness) of mid-column for M1, M2 and M3, derived from NS

The NSA results are shown in **Figure 5**, detailing force and displacement values, while **Figure 6** compares NSA and NDA outcomes. Notation Mi,s indicates drift values from NSA, and Mi,d denotes those from NDA. The analysis reveals that the mid-columns in M2 and M3, designed with higher ductility, perform better in damage tolerance than M1. Differences in cross-sectional shapes and

reinforcement also impact their responses to loading. M1, with massive mid-columns designed as DCL, shows the lowest drift values for SD and MD states, indicating robust performance. In contrast, M2 and M3, designed as DCM, exhibit higher drift values, especially in ED and CD states, suggesting reduced structural integrity under severe conditions. While M2 has lower drift than M3 for ED and CD, both surpass M1, highlighting the significance of design in mitigating damage. M1 requires less force than M2 to reach ED and CD states, indicating it is more resilient initially but less robust overall compared to M2, which demands the highest force to reach damage states, reflecting its superior capacity. M3 performs well in the ED state but is less effective than M2 in the CD state, requiring less force than M2 while outperforming M1 in certain cases.

3.2 Fragility analysis results

Fragility curves give insights into the probability of exceeding certain damage limit states (SD, MD, ED, CD) under varying ground motion PGA (Peak Ground Acceleration). The results of the analysis are shown in **Figure 7**.

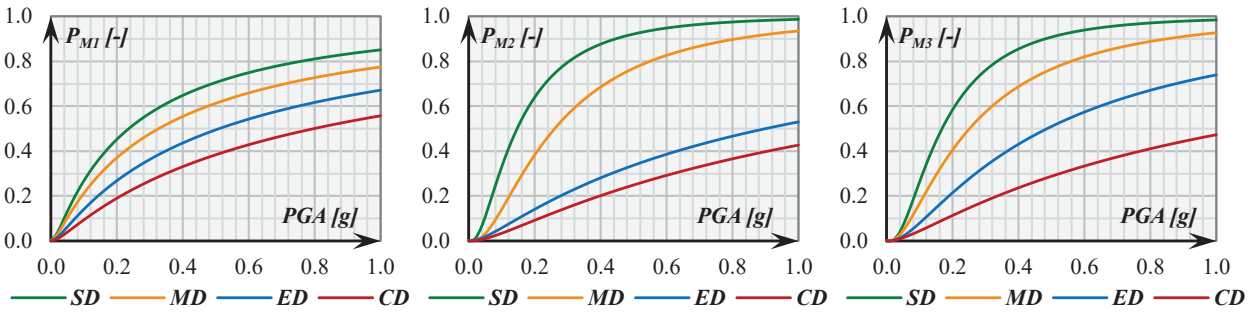

Figure 7: Fragility curves for M1, M2 and M3 for damage LS: SD, MD, ED, CD

Fragility curves are calculated as the empirical fragility curves. An empirical fragility function is one that is created by fitting a function to approximate observational data. The observational data in this case represents number of assets exposed to some level of excitation, and the number of those that failed when subjected to the environmental excitation (i.e., reaching or exceeding the specified limit state). The set of the obtained probability points is fitted for each DS using the Maximum Likelihood Estimation (MLE) method described in [17].

$$\text{Likelihood} = \prod_{j=1}^{m} \binom{n_j}{Z_j} \phi\left(\frac{\ln(\frac{IM_j}{\theta_{DS_i}^{IM}})}{\beta_{LN|DS_i}^{IM}}\right)^{Z_j} \left[1 - \phi\left(\frac{\ln(\frac{IM_j}{\theta_{DS_i}^{IM}})}{\beta_{LN|DS_i}^{IM}}\right)\right]^{n_j - Z_j} \tag{1}$$

where m is the total number of IM levels, $\theta_{DS_i}^{IM}$ is the mean value of distribution in arithmetic space and $\beta_{LN|DS_i}^{IM}$ is the value of the standard deviation in logarithmic form of the lognormal cumulative probability distribution function of the fitted fragility curve for the reference value of the IM for the corresponding damage state, 1 DS. Probability for the exceedance of different states of damage for the design PGA of 0.1g is calculated using the equations described in research in [17].

$$
\begin{aligned}
P_{DS_0} &= 1 - P_{DS_1}[IM_j, \mu_{LN|DS_1}, \sigma_{LN|DS_1}] \\
P_{DS_i} &= P_{DS_i}[IM_j, \mu_{LN|DS_i}, \sigma_{LN|DS_i}] - P_{DS_{i+1}}[IM_j, \mu_{LN|DS_{i+1}}, \sigma_{LN|DS_{i+1}}] \\
P_{DS_n} &= P_{DS_n}[IM_j, \mu_{LN|DS_n}, \sigma_{LN|DS_n}]
\end{aligned} \tag{2}
$$

where P_{DS_0} is the probability of no damage to occur and $i = 1, ..., n$ and $IM_j = (0 - 1.0g$. i is an index of a particular DS, and j is an index of a particular IM (PGA). n is the total number of damage states.

The fragility analysis highlights significant differences among the models regarding damage probabilities under various seismic intensities. Model M1 exhibits higher susceptibility to damage, particularly at higher ground accelerations, while M2 and M3 show enhanced resilience. At higher PGA levels, M1's damage probabilities rise more rapidly, approaching 1.0 sooner than M2 and M3, indicating greater vulnerability to extreme seismic events. In contrast, M2 and M3 display a leveling off of probabilities, suggesting they can endure more intense shaking before experiencing extensive damage. This suggests that M1 may require retrofitting to improve its performance, whereas M2 and M3 could benefit from design optimizations. Overall, M1 is the most vulnerable model, suitable for lower seismic risk areas. M2 and M3, particularly M3, are better choices for regions with higher seismicity, emphasizing robustness in design to minimize damage during seismic events.

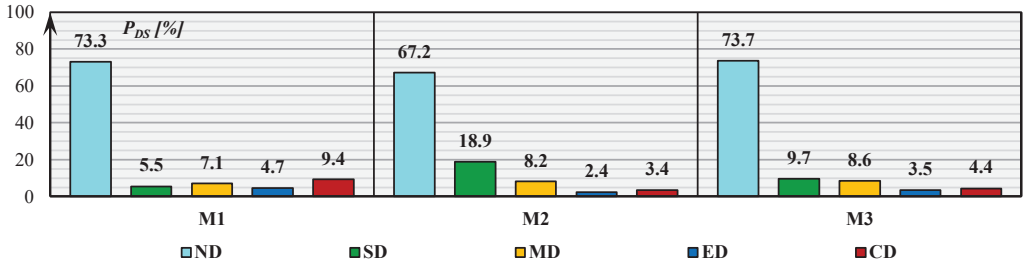

Figure 8: Probability of the exceedance of different states of damage for the design PGA of 0.1g for M1, M2 and M3

At a design PGA of 0.1g (**Figure 8**), M1 requires the highest force in the no damage (ND) state, indicating strong initial resilience, but it shows moderate drift in SD and MD and significant drift in ED and CD states, revealing vulnerability under extreme conditions. M2 has a lower ND force requirement and higher drift in the SD state, suggesting sensitivity to initial damage, yet it performs better in ED and CD states, maintaining structural integrity. M3 demonstrates balanced performance with moderate drift in SD and MD states and relatively high force requirements in ND and SD, showing good initial capacity but slightly less resilience in extreme scenarios. Overall, M2 performs best in extreme conditions, M1 in the no damage state, and M3 offers a balanced resilience across damage states, highlighting the impact of design parameters on structural performance.

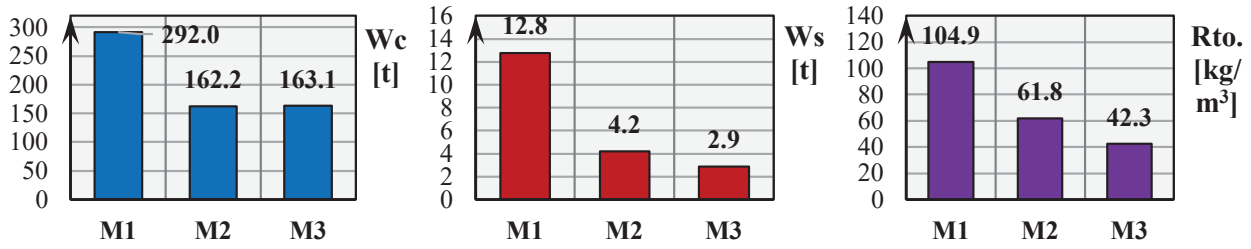

Figure 9: Comparation of materials and their ratio for M1, M2 and M3 in tons and kg/m3

3.3 Material quantity analysis

Material quantities used in the three bridge models (M1, M2, and M3) to assess their efficiency and structural performance are compared. Understanding material usage is crucial for evaluating economic, sustainability, and seismic resilience aspects. **Figure 9** shows the differences in concrete and reinforcement requirements. M1 uses the most concrete and reinforcement, indicating a substantial design. M2 is more efficient, using less concrete while maintaining robustness. M3 matches M2 in concrete volume but slightly exceeds it in mass, reflecting balanced material usage. M1's high rebar-to-concrete ratio enhances strength but may be less efficient, while M2 optimizes this ratio for strong performance. M3, using the least reinforcement, is material-efficient but may lack the resilience of M1 and M2 in extreme conditions.may lack the resilience of M1 and M2 in extreme conditions.

4 Final remarks and recommendations

This analysis shows the need for seismic assessments of existing reinforced concrete road bridges, particularly those not compliant with current standards. The findings indicate that many structures are vulnerable to significant damage during severe earthquakes, which can jeopardize their functionality and safety. Key components such as pier columns, abutments, and bearings should be prioritized in evaluations, as they are most susceptible to damage. The comparative analysis of the three reinforced concrete bridge models demonstrates significant variations in seismic resilience and performance based on design choices. M1, while initially robust, shows vulnerability under extreme seismic events due to its higher susceptibility to damage. In contrast, M2 and M3 exhibit superior resilience, particularly in extensive and complete damage states, underscoring the importance of ductility in design. The fragility curves further illustrate these differences, with M2 proving most effective in extreme conditions, suggesting its suitability for higher seismic zones. The study highlights the essential importance of design parameters in improving bridge performance and underscores the need for continuous optimization to address seismic risks.

5 References

[1] Motter, C., Philips, A.: Data - driven assessment of post-earthquake bridge functionality and regional mobility, PacTrans, WSDOT, Washington State University

[2] Priestley M.J.N, Seible F, Calvi G.M, (1996): Seismic design and retrofit of bridges, John Wiley & Sons Inc, NY.

[3] EN 1998-2: European Committee for Standardization. (2005). Eurocode 8: Design of structures for earthquake resistance. Part 2: Bridges. EN 1998-2:2005.

[4] Cao, Y., Liang, Y., Huai, C. Yang J., Mao, R.: Seismic Fragility Analysis of Multispan Continuous Girder Bridges with Varying Pier Heights considering Their Bond-Slip Behavior, Advances in Civil Engineering, (2020), Article ID 8869921

[5] Hong, Y., Ye, L., Xie, W.,: Seismic Fragility and Resilience improvement of convential Bridges supported by double-column piers utilizing shear links, Structures 57, 2023; 105309

[6] Sayyed,A.G., Pawar„ P.M., Study on Fragility Analysis of RC Bridges in India, Int. Res. J. of Eng. and Technology (IRJET), Vol. 08 Issue 12, Dec. 2021. www.irjet.net

[7] Zhang, Qi, Alam, M.S.: Performance-based seismic design of bridges: a global perspective and critical review of psst, present and future direction, Structure and Inrfa. Eng. 2018, P 1558269.

[8] Palermo, A., Mashad, M.: Accelerated bridge construction (ABC) and seismic damage resistant technology: a New Zealand challenge, Bulletin NZ SEE, Vol.45, No.3, 2012.

[9] EN 1990: European Committee for Standardization. (2002). Eurocode - Basis of structural design. EN 1990:2002.

[10] EN 1991: European Committee for Standardization. (2002). Eurocode 1: Actions on structures. Part 1-1: General actions - Densities, self-weight, imposed loads for buildings. EN 1991-1-1:2002.

[11] EN 1992-2: European Committee for Standardization. (2005). Eurocode 2: Design of concrete structures. Part 2: Concrete bridges - Design and detailing rules. EN 1992-2:2005.

[12] Radimpex Tower, Software for Structural Analysis and Design

[13] Computers and Structures, Inc., SAP2000: Structural Analysis and Design Software

[14] Seismosoft SeismoStruct: Structural Analysis Software for Seismic Design

[15] Čokić M., Folić R., Folić B., Robustness assessment of RC buildings by analysis of fragility and vulnerability, Structures, Volume 62, 2024, 106107, ISSN 2352-0124

[16] ORFEUS - Observatories & Research Facilities for European Seismology. Retrieved: September 2024, from https://www.orfeus-eu.org/

[17] Porter, K. A Beginner's Guide to Fragility, Vulnerability, and Risk; University of Colorado Boulder: Boulder, CO, USA, 2015;